High magnetic field spin splitting of excitons in asymmetric GaAs quantum wells

J. Jadczak, M. Kubisa,* K. Ryczko, and L. Bryja
Institute of Physics, Wrocław University of Technology, Wybrzeże Wyspiańskiego 27, 50-370, Wrocław, Poland

M. Potemski
Laboratoire National des Champs Magnétiques Intenses, CNRS-UJF-UPS-INSA, Grenoble, France
(Received 6 October 2012; published 3 December 2012)

Low-temperature photoluminescence from high-quality GaAs quantum wells, asymmetrically doped with carbon, are investigated under high magnetic fields (up to 20 T) directed along the [001] growth axis. At higher fields, in the σ^- polarized emission, we observe two well-resolved lines which are attributed to the recombination of neutral (X) and charged (X^+) excitons. In contrast, only the neutral exciton line is observed for the σ^+ polarization. From the difference of the X line positions for the two polarizations we determine the effective Zeeman splitting of neutral excitons and then the g factor g_h of confined holes. We find that g_h depends substantially on the well size and changes the sign at moderate magnetic fields. To explain the experimental results, the valence Landau levels are calculated using the Luttinger model beyond the axial approximation. We demonstrate that mainly the excited hole levels contribute to the excitonic state at higher magnetic fields. Due to their light-hole character, resulting from the valence-band mixing, the excited hole states have a sizable overlap with the electron states confined far from the doped barrier. The calculated values of g_h are in an excellent quantitative agreement with the experimental data.

DOI: 10.1103/PhysRevB.86.245401 PACS number(s): 73.21.Fg, 72.25.Fe

I. INTRODUCTION

Excitons which dominate the optical spectra of two-dimensional systems have been intensively studied during the last decades. However, the spin structure of bound electron-hole complexes has received only a marginal attention from researchers. It used to be assumed that the exciton spin splitting was unaffected by the interaction between charged particles. Recent observations of an anomalous magnetic field dependence of the g factors for neutral and charged excitons[1–4] have revised this opinion and revealed some open issues. Furthermore, the spin properties of exciton complexes have currently attracted considerable interest due to their possible applications in the field of spintronics.[5]

The spin splitting of excitons in GaAs quantum wells was investigated using different experimental methods, such as polarization-resolved photoluminescence,[1,2,4,6–8] quantum-beat spectroscopy,[9,10] spectral hole burning technique,[11] magnetoreflectance,[12] reflectance difference spectroscopy,[13] optically detected magnetic resonance,[14,15] and spin-flip Raman scattering.[16] Even early measurements[6,7] revealed that the Zeeman splitting of heavy-hole excitons, linear in a magnetic field B in narrow wells, departs from linearity as the well width exceeds approximately 10 nm. In particular, the exciton g factor in wide structures was shown to exhibit a sign reversal as a function of B. Glasberg *et al.*[2] investigated the spin splitting of both neutral and charged excitons measured within the same wide quantum well. They observed that the g factors of all exciton complexes strongly depend on the magnetic field and change sign as the field is increased. Moreover, the Zeeman splittings of charged and neutral excitons were found similar at very low fields but significantly different at larger B.

The nonlinear behavior of the exciton spin splitting was explained as due to the effect of valence-band mixing which modifies the hole g factor. Indeed, the state of the hole involved in the exciton is not a pure heavy-hole state, but contains an admixture of a light-hole component which increases with an increasing magnetic field. And since the heavy and light holes have very different g factors, the exciton spin splitting changes nonlinearly with B, which corresponds to a field-dependent effective g factor. The mixing is especially effective in wide quantum wells, where the energy splitting between the valence subbands is small. Traynor *et al.*[8] compared the low-field exciton g factors, measured for a series of quantum wells with different widths, with the results of eight-band $k \cdot p$ calculations, which included the valence-band mixing but ignored the Coulomb coupling of the electron and hole. They found a good agreement only for the narrowest wells, where the sign reversal of g is not observed. For the wider wells the theory predicted the sign inversion, however, at much lower magnetic fields than observed experimentally. More detailed calculations[17,18] showed that the electron-hole interaction shifts the crossing of the exciton ground states (which results in the sign reversal of g) towards higher magnetic fields. Nevertheless, the calculated values of the crossing field were significantly higher than observed in the experiment. In a recent work, Castelano *et al.*[4] extended the theory to include both neutral and charged excitons. They also considered the GaAs quantum wells grown along two different crystal directions. The results agreed qualitatively with the experimental data in the case of the [110] well, however, the calculated crossing fields were about two times higher than the measured ones. Unfortunately, for the [001] wells, the theory of Castelano *et al.* was inconsistent, even qualitatively, with the results of Ref. 2. Therefore, although a consensus exists that the nonlinear behavior of the exciton Zeeman splitting results from the valence-band mixing, the mechanism of this effect is still not fully understood.

The works cited above consider excitons in undoped heterostructures under low or moderate magnetic fields. In the present paper we investigate the high-field exciton Zeeman

splitting in p-doped GaAs quantum wells of different widths. The built-in electric field present in doped structures is known to change the subband energies and to reduce the excitonic binding due to the spatial separation of electrons and holes. We show that it also modifies the spin properties of confined excitons. Polarization-resolved photoluminescence measurements are used to determine the exciton Zeeman splitting and the g factor of holes. The experimental results are compared with detailed band-structure calculations based on the Luttinger model. Our theory includes a realistic model of charge distribution in doped quantum wells and the effects of the cubic anisotropy of hole subbands. We show that in wide asymmetric wells the spin properties of the heavy-hole excitons are governed by the excited valence-band Landau levels with a light-hole character. The calculated g-factor values are in excellent agreement with the experimental data.

II. SAMPLE DETAILS AND EXPERIMENT

We have examined a selection of high-quality asymmetrically doped quantum wells with widths w of 18, 22, and 25 nm. The structures were grown by molecular beam epitaxy (MBE) on a (001)-oriented semi-insulating GaAs substrate, employing the following growth sequence: 100 nm GaAs, 5 nm AlAs, 200 nm GaAs, 150 nm $Ga_{0.65}Al_{0.35}As$, the superlattice consisting of 33 repetitions of 2 nm GaAs and 1 nm AlAs, 57 nm $Ga_{0.65}Al_{0.35}As$, w-wide GaAs quantum well, 40 nm $Ga_{0.65}Al_{0.35}As$, carbon δ-doping, 80 nm $Ga_{0.65}Al_{0.35}As$, and the 5 nm carbon δ-doped GaAs cap. The low-temperature hole mobility $\mu \approx 10^5$ cm^2/V·s was nearly the same for all samples. The quantum Hall effect measured in the van der Pauw geometry (concurrently with the photoluminescence) was used to estimate the concentration p of holes. In the dark, p varied slightly from sample to sample in the range of 1.8–2.4 $\times 10^{11}$ cm^{-2}. Under laser illumination, the concentration decreased linearly with an increase of the excitation power density. In the actual experimental conditions, however, p has changed by less than several percent.

Photoluminescence (PL) was excited by the red 720-nm line of a titanium sapphire tunable laser with the photon energy below the barrier band gap. The measurements were performed in a bath liquid helium cryostat, at temperatures varying from $T = 1.8$ to 4.2 K. The magnetic field applied in the Faraday configuration was changed with a small step $\Delta B = 0.05$ T, up to the maximum value of $B = 20$ T. We used a fiber-optic system with a linear polarizer and a quarter-wave plate placed close to the sample. The σ^- and σ^+ helices were switched by reversing the field direction. The spectra were analyzed using the 1.0-m long monochromator and a nitrogen-cooled CCD camera.

III. RESULTS AND DISCUSSION

A. PL spectra in high magnetic fields and the determination of hole g factor

For zero magnetic field a single line was observed in the photoluminescence spectra of all investigated samples, independent of the laser excitation power. This observation is in contrast to our previous studies of a symmetrically doped 15-nm quantum well with a similar concentration of two-dimensional (2D) holes.[19] In the symmetric structure, at a low excitation power, we also observed a single PL peak which was attributed to positively charged excitons. However, as the excitation level was increased, an additional line appeared at higher energies, which resulted from the neutral exciton recombination. In the case of the asymmetric wells studied here, a similar double-peak structure was observed only at high magnetic fields (above 6 T). Furthermore, as can be seen in Fig. 1, the second line appeared only in the σ^- polarized emission.

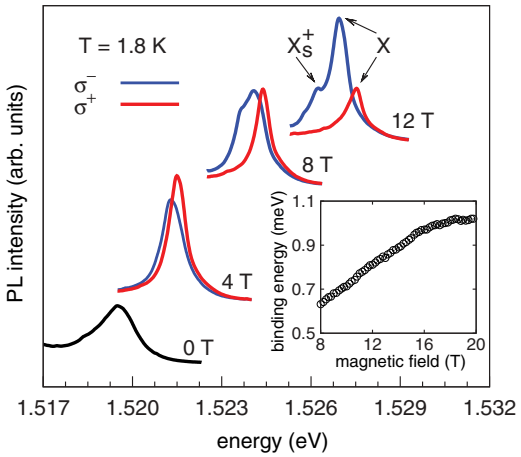

FIG. 1. (Color online) Photoluminescence from the 25-nm well measured at selected magnetic fields in different circular polarizations. Inset shows the trion binding energy determined in the σ^- polarization.

Figure 1 presents the magnetic field evolution of the PL spectra of the 25-nm well, which is representative for all studied samples. We attributed the lines observed in the σ^- polarization to the recombination of positively charged excitons in the singlet state (X_s^+, the lower-energy peak) and to that of neutral excitons (X, the higher-energy peak). The magnetic field dependence of the trion binding energy, determined from the splitting of the two lines, is shown in the inset to Fig. 1. The binding energy of X_s^+ state is significantly smaller than that observed in symmetric structures,[19] and consistent with the results of theoretical calculations[20] performed for similar asymmetric structures. By the extrapolation of experimental data to zero magnetic field we found that the trion binding energy quickly vanishes and the additional hole becomes unbound as the field is decreased. This explains the observation of a single peak in the low-field PL spectra and supports our interpretation of the observed lines. In the σ^+ polarization a single peak was observed for all fields up to 20 T and was attributed to the neutral exciton recombination. Trion emission was not observed in this polarization.

From the energy difference between the exciton lines in both polarizations, we determined the effective g factor g_X of neutral excitons using the equation

$$\Delta E_X = E_X(\sigma^+) - E_X(\sigma^-) = \mu_B g_X B, \qquad (1)$$

where μ_B is the Bohr magneton. Our description of the spin properties of free carriers and excitons is based on the notation and sign conventions proposed recently by Bartsch *et al.*[21] This schematic is quite similar to that proposed by van Kersten *et al.*[14] The only difference is that the sign of the g factors

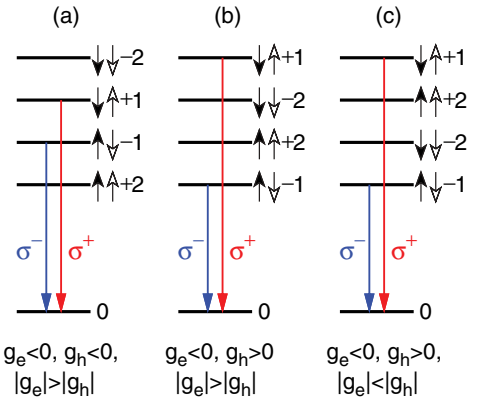

FIG. 2. (Color online) The scheme of the spin structure and optical transitions (emission) for neutral excitons in external magnetic fields. Short arrows show carriers spin, filled for electrons and empty for holes. The total spin of each state is additionally given by numbers.

for the hole and exciton are reversed. The schematic diagram of the optical transitions for the recombination of heavy-hole excitons is given in Fig. 2. We see that the effective g factor for the bright exciton with spin ± 1 is

$$g_X = g_h - g_e, \tag{2}$$

independent of the mutual size of the electron (g_e) and hole (g_h) g factors. Equation (2) allows to determine the g factor for confined holes from the experimental values of g_X. The electron g factor was evaluated using the well-established empirical formula[22]

$$g_e(E) = -0.445 + 3.38 \cdot (E - 1.519) - 2.21 \cdot (E - 1.519)^2, \tag{3}$$

where E (in eV) is the transition energy. The final results are presented in Fig. 3(b). For all studied samples g_h increases with increasing magnetic field and tends to saturate at the highest values of B. The hole g factor is negative in low fields and changes to positive at some value of B, which depends on the well size.

B. Theoretical framework

To explain the observed properties of the hole spin splitting we evaluated the energies and wave functions of carriers confined in the investigated structures. The Landau levels of two-dimensional electrons and holes were calculated using the numerical method, developed previously[23] for p-doped single heterojunctions and adapted for quantum wells. As a first step, the energies of the hole subbands and the potential distribution $V(z)$ in the well were determined by self-consistently solving the Schrödinger and Poisson equations at zero magnetic

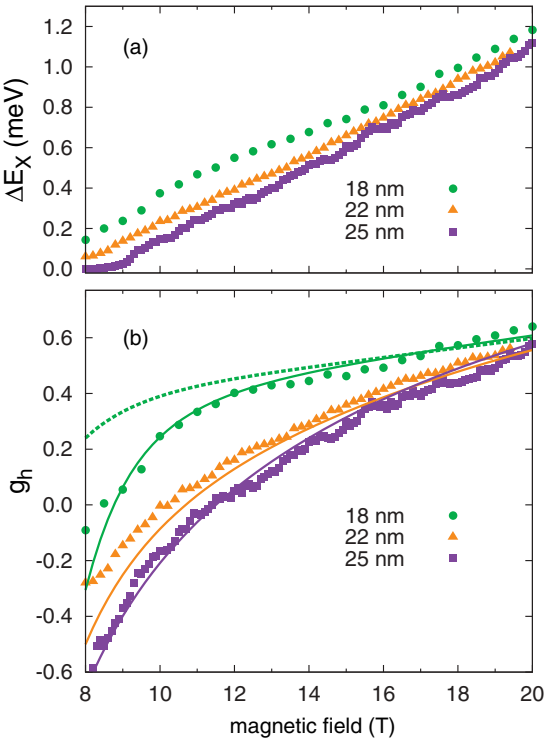

FIG. 3. (Color online) (a) Measured magnetic field dependence of exciton spin splitting. (b) Hole g factor calculated (solid lines) and measured experimentally (symbols) in the investigated samples as a function of the magnetic field. Dotted line shows the results obtained in the axial approximation for the 18-nm well.

field. The contribution of mobile holes to the potential was calculated in the Hartree approximation and the hole states were represented by exact eigenfunctions of the Luttinger Hamiltonian. The potential created by the immobile charge was computed assuming that the background doping of MBE-grown GaAs is of p type. We used the following values of valence-band parameters[24] $\gamma_1 = 6.85$, $\gamma_2 = 2.10$, $\gamma_3 = 2.90$, and $\kappa = 1.2$ for GaAs and $\gamma_1 = 3.45$, $\gamma_2 = 0.68$, $\gamma_3 = 1.29$, and $\kappa = 0.12$ for AlAs. Linear interpolation was applied for $Al_xGa_{1-x}As$. The value of the valence-band offset was determined as 35% of the difference in band gaps in two adjacent layers. The concentration of residual donors was taken to be 5×10^{14} cm^{-3}.

In the next step, the potential $V(z)$ was used to calculate the energies and wave functions of hole Landau levels in the magnetic field normal to the quantum well plane. To improve the accuracy of results, the calculations were extended beyond the axial approximation employed in Ref. 23. The Luttinger Hamiltonian was written as the sum $H = H_{ax} + H_{\rm cub}$, with the axial and cubic parts given by

$$H_{ax} = -\frac{\hbar^2}{2m_o L^2} \begin{bmatrix} p+q+\frac{3}{2}\kappa & l & m & 0 \\ l^+ & p-q+\frac{1}{2}\kappa & 0 & m \\ m^+ & 0 & p-q-\frac{1}{2}\kappa & -l \\ 0 & m^+ & -l^+ & p+q-\frac{3}{2}\kappa \end{bmatrix} + V(z), \tag{4a}$$

and

$$H_{\text{cub}} = -\frac{\hbar^2}{2m_o L^2}\begin{bmatrix} 0 & 0 & r & 0 \\ 0 & 0 & 0 & r \\ r^+ & 0 & 0 & 0 \\ 0 & r^+ & 0 & 0 \end{bmatrix}, \tag{4b}$$

where

$$\begin{aligned} &p = \gamma_1\left(a^+a^- + \frac{1}{2} + \frac{1}{2}L^2K_z^2\right), \quad q = \gamma_2\left(a^+a^- + \frac{1}{2} - L^2K_z^2\right), \quad l = -i\sqrt{6}\gamma_3 L K_z a^-, \\ &m = \frac{\sqrt{3}}{2}(\gamma_2 + \gamma_3)(a^-)^2, \quad r = \sqrt{\frac{3}{2}}(\gamma_2 - \gamma_3)(a^+)^2. \end{aligned} \tag{4c}$$

Here $\vec{K} = -i\vec{\nabla} + (e/\hbar c)\vec{A}$ is the kinetic momentum operator, $\vec{A}$ is the vector potential, $a^{\mp} = (L/\sqrt{2})(K_x \mp iK_y)$ are the creation and destruction operators, $L = \sqrt{\hbar c/eB}$ is the magnetic length, and m_0 is the free-electron mass. At first, we solved the Schrödinger equation for the axial Hamiltonian

$$H_{ax}\Psi_n^{ax} = E_n^{ax}\Psi_n^{ax}, \tag{5}$$

using the transfer matrix method introduced in Ref. 23. The axial eigenvectors have the form

$$\Psi_n^{ax} = \begin{bmatrix} F_1(z)\phi_{n-1} \\ F_2(z)\phi_n \\ F_3(z)\phi_{n+1} \\ F_4(z)\phi_{n+2} \end{bmatrix}, \tag{6}$$

where the harmonic oscillator functions ϕ_n satisfy $a^+\phi_n = \sqrt{n+1}\phi_{n+1}$ and $a^-\phi_n = \sqrt{n}\phi_{n-1}$. The index n runs over the values $n = -2, -1, 0, 1, \ldots$ and the envelope functions $F_j(z)$ are automatically zero for those components which have harmonic oscillator functions ϕ_n with n negative. Next, the accurate hole energies were calculated by treating the cubic Hamiltonian, Eq. (4b), as a perturbation. We diagonalized the Hamiltonian matrix

$$H_{mn} = \left\langle \Psi_m^{ax} \middle| H \middle| \Psi_n^{ax} \right\rangle = E_n^{ax}\delta_{mn} + \left\langle \Psi_m^{ax} \middle| H_{\text{cub}} \middle| \Psi_n^{ax} \right\rangle, \tag{7}$$

written in the basis of axial states Ψ_n^{ax}, which were regarded as near-degenerate states. An inspection of Eq. (6) shows that H_{cub} couples the axial Landau levels with n differing by 4. The accuracy of calculations was checked by varying the number of axial states used in the diagonalization.

C. Analysis and discussion of results

Figure 4(a) presents the calculated magnetic field dependence of the energies of the topmost valence-band levels in the 25-nm well. All the states shown in the graphic belong to the ground heavy-hole subband. They are labeled by the index n of the largest axial component of the wave function. For $n \geqslant +1$ there are two axial levels with the same number n in each subband, distinguished by the letters a and b. Colors mark the optically active states, from which holes can recombine with photoexcited electrons with the emission of σ^- (blue) or σ^+ (red) polarized light.[23] Since the number of photoexcited electrons is small, they all occupy only the $n = 0$ conduction band Landau level.

It seems natural to assign the transitions observed in our low-temperature photoluminescence spectra to the optically active hole states with the highest energies. However, the g factor calculated from the energy difference of the levels $1a$ and -2 is significantly greater than the measured one and positive in the whole range of magnetic fields. Surprisingly, g_h obtained from the experiment agrees well with the energy splitting of hole states with somewhat lower energy. The full lines in Fig. 3(b) show the g factor determined from the energy difference of the hole levels $1b$ and -1. The calculated values closely reproduce the measured dependence of the hole spin splitting on both the magnetic field and the size of the well. It is therefore clear that the observed optical transitions involve excited hole Landau levels and not the ground ones.

This feature can be understood from the excitonic character of the transitions. In a simple model, excitonic transitions in the limit of strong magnetic fields can be regarded as Landau level transitions perturbed by the Coulomb interaction between electron and hole.[25] A larger overlap of electron and hole states results in a larger Coulomb coupling, and thus, in a larger exciton binding energy. An inspection of the envelope functions for the topmost valence-band levels, presented in Fig. 4(c), shows that the ground states $1a$ and -2 are localized near the doped barrier, whereas the excited states $1b$ and -1 are localized much closer to the center of the well. Therefore, the excited hole states have a larger overlap with the electron wave function shown in Fig. 4(b).

We made an estimation of the binding energies of the excitons associated with the hole states shown in Fig. 4(c). Calculations were based on the adiabatic method proposed by Leavitt and Little[26] and later extended by Peyla *et al.*[27] to include magnetic fields. The exciton binding energy was calculated as

$$E_b = \int_{+\infty}^{-\infty} dz_e \int_{+\infty}^{-\infty} dz_h |f(z_e)|^2 |f(z_h)|^2 |E^{2D}(z_e - z_h, B)|, \tag{8a}$$

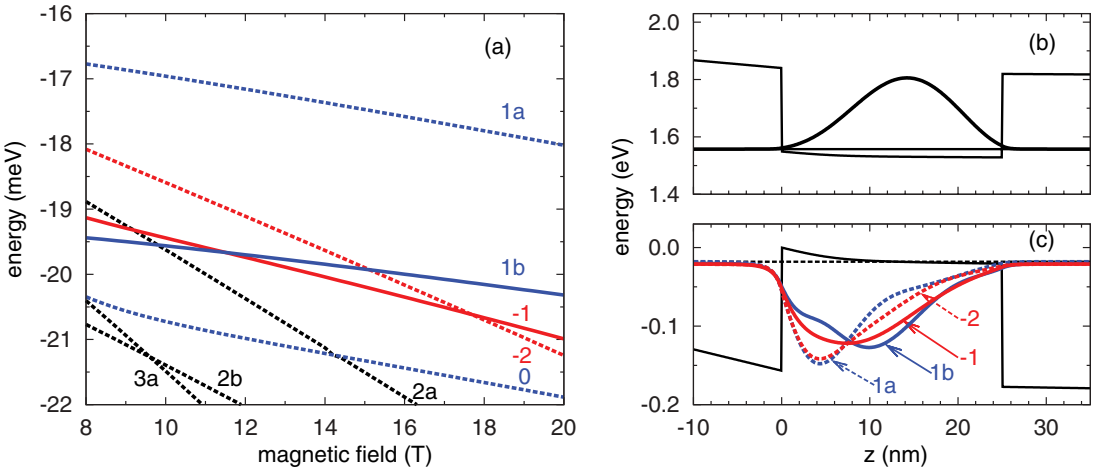

FIG. 4. (Color online) (a) Calculated energies and (c) envelope functions of the topmost hole Landau levels in the 25-nm well. Colors mark the optically active states in the σ^- (blue) and σ^+ (red) polarizations. Panel (b) shows the envelope function of conduction band electrons.

where f_e and f_h are the electron and hole envelope functions, respectively [f_h was approximated by the optically active component of vector (6)], and $E^{2D}(Z,B)$ is the ground eigenvalue of the two-dimensional Hamiltonian

$$H^{2D} = -\frac{\hbar^2\nabla_{||}^2}{2\mu_{||}} - \frac{e^2}{4\pi\epsilon\sqrt{\rho^2+Z^2}} + \frac{e^2B^2}{8\mu_{||}}\rho^2. \qquad (8b)$$

Here $\rho = |\vec{\rho}_e - \vec{\rho}_h|$ and $Z = |z_e - z_h|$ are the relative electron-hole coordinates, $\vec{\nabla}_{||}$ is the component of the gradient with respect to ρ, and $\mu_{||}$ is the in-plane reduced effective mass. For the 25-nm shown in Fig. 4 at the magnetic field $B = 20$ T, we obtained the following values of the binding energy: 11.7 meV (*1a* exciton), 15.8 meV (*1b*), 12.8 meV (*-2*), and 14.4 meV (*-1*). Clearly the 1*b* (*-1*) exciton has a lower energy than the 1*a* (*-2*) one since the gain in binding energy due to the larger overlap exceeds the energy difference between the hole levels involved in different excitonic states. That is why the excitons related to the excited hole levels are observed in the low-temperature photoluminescence.

The simplified picture of excitonic transitions as the Coulomb-perturbed Landau level transitions is not really justified under our experimental conditions. Since the exciton binding energy exceeds the Landau splitting of hole levels, the true exciton state contains a mixture of topmost valence band states. One can expect, however, that the excited levels 1*b* and -1 will dominate the exciton state because of their larger overlap with the electron state.

The calculated results, shown in Fig. 3(b), reproduce remarkably well the g factor measured in all investigated samples, in particular at higher magnetic fields. At lower fields and in the narrower wells the agreement with experiment decreases. This is due to the fact that as the field is reduced, the envelope functions of all heavy-hole levels become similar and they contribute equally to the excitonic state. For this reason, in low magnetic fields, the Zeeman splitting of exciton emission cannot be related to the energy splitting of a single pair of valence Landau levels.

Our theory shows that the characteristic features of the exciton spin splitting observed in the experiment, such as the change of sign of g factor and its saturation at the largest fields, result from a peculiar behavior of hole Landau levels. To reproduce the experimental results, it was necessary to perform detailed calculations of the valence band states in a doped quantum well. In particular, as can be seen in Fig. 3(b), the inclusion of the usually ignored cubic terms in the Luttinger Hamiltonian significantly improved the agreement with experiment.

The results presented here clearly confirm the effect of valence-band mixing on the exciton Zeeman splitting. The excited hole levels 1*b* and -1, which were shown to govern the exciton g factor at high magnetic fields, have light-hole character even though they belong to the ground heavy-hole subband. And because of a small effective mass, their envelope functions extend over the whole well and overlap significantly with the electron states. The effect of valence-band mixing is most important for wide quantum wells and becomes negligible for narrow ones, as the energy separation between the heavy- and light-hole subbands increases. Furthermore, as the electron-hole distance decreases in narrow wells, the electron-hole overlap becomes comparable for valence states of the light- and heavy-hole types.

Our theory concerns asymmetric heterostructures and cannot be directly applied to undoped quantum wells studied in the previous works.[1–4,6–18] However, some remarks can be made with regard to these systems. Previous calculations[4,8,17,18] of the exciton spin splitting used the simple rectangular well model. In a rectangular well, all states in the ground valence subband are localized at the well center and have a similar overlap with the electron state. Therefore, the spin properties of excitons are governed by the valence levels of heavy-hole character, with higher energies. The rectangular well model is, however, not very realistic. Indeed, a p-type background doping, although small, is present in nominally undoped MBE-grown heterostructures. It produces a band bending, which localizes the states of heavy-hole type closer to the interfaces, and thus removes them from the electron state. Besides, in recent experiments[2,4] laser illumination was used to generate excess carriers in the quantum well structures. This produced an additional electric field which further separated

the electrons and holes.[2] The above factors, which influence the shape of the well, should be taken into account in realistic calculations of the exciton spin splitting. Our results clearly show that the *g* factor of exciton is very sensitive to the spatial distribution of potential.

IV. CONCLUSION

We investigated both experimentally and theoretically the exciton spin in asymmetrically doped quantum wells under high magnetic fields. The nonlinear field behavior of spin splitting and its dependence on the well size, observed in the photoluminescence measurements, were explained as the results of the valence-band mixing. In particular, we demonstrated that at high fields the properties of heavy-hole excitons are governed by the excited hole Landau states which have light-hole character. Excellent agreement was obtained between the theory and experiment. The observed dependence of spin splitting on the potential profile across the structure suggests that an external electric field (applied, e.g., using a gate bias) can be used as a simple tool to manipulate the exciton spin.

ACKNOWLEDGMENTS

The structures used in the experiment have been kindly supplied to us by D. Reuter and A. Wieck. The work was supported by Polish MNiSW Grant No. N202179538 and EuroMag-NET II under EU Contract No. 228043.

*Maciej.Kubisa@pwr.wroc.pl

[1] V. B. Timofeev, M. Bayer, A. Forchel, and M. Potemski, JETP Lett. **64**, 57 (1996).
[2] S. Glasberg, G. Finkelstein, H. Shtrikman, and I. Bar-Joseph, Phys. Rev. B **59**, R10425 (1999).
[3] V. Kochereshko, L. Besombes, H. Mariette, T. Wojtowicz, G. Karczewski, and J. Kossut, Phys. Status Solidi B **247**, 1531 (2010).
[4] L. K. Castelano, D. F. Cesar, V. Lopez-Richard, G. E. Marques, O. D. D. Couto, F. Iikawa, R. Hey, and P. V. Santos, Phys. Rev. B **84**, 205332 (2011).
[5] For a recent review see M. M. Glazov, Phys. Solid State **54**, 1 (2012).
[6] W. Ossau, B. Jäkel, E. Bangert, and G. Weimann, in *Properties of Impurity States in Superlattice Semiconductors*, NATO Advanced Study Institutes, Series B: Physics, Vol. 183, edited by C. Y. Fong, Inder P. Batra, and C. Cirac (Plenum, New York, 1988), p. 285.
[7] M. J. Snelling, E. Blackwood, C. J. McDonagh, R. T. Harley, and C. T. B. Foxon, Phys. Rev. B **45**, 3922 (1992).
[8] N. J. Traynor, R. J. Warburton, M. J. Snelling, and R. T. Harley, Phys. Rev. B **55**, 15701 (1997).
[9] O. Carmel, H. Shtrikman, and I. Bar-Joseph, Phys. Rev. B **48**, 1955 (1993).
[10] R. E. Worsley, N. J. Traynor, T. Grevatt, and R. T. Harley, Phys. Rev. Lett. **76**, 3224 (1996).
[11] H. Wang, M. Jiang, R. Merlin, and D. G. Steel, Phys. Rev. Lett. **69**, 804 (1992).
[12] P. Lefebvre, B. Gil, J. P. Lascaray, H. Mathieu, D. Bimberg, T. Fukunaga, and H. Nakashima, Phys. Rev. B **37**, 4171 (1988).
[13] Y. H. Chen, X. L. Ye, B. Xu, Z. G. Wang, and Z. Yang, Appl. Phys. Lett. **89**, 051903 (2006).
[14] H. W. van Kesteren, E. C. Cosman, W. A. J. A. van der Poel, and C. T. Foxon, Phys. Rev. B **41**, 5283 (1990).
[15] P. G. Baranov, I. V. Mashkov, N. G. Romanov, P. Lavallard, and R. Planel, Solid State Commun. **87**, 649 (1993).
[16] V. F. Sapega, M. Cardona, K. Ploog, E. L. Ivchenko, and D. N. Mirlin, Phys. Rev. B **45**, 4320 (1992).
[17] G. E. W. Bauer and T. Ando, Phys. Rev. B **37**, 3130 (1988).
[18] G. E. W. Bauer and T. Ando, Phys. Rev. B **38**, 6015 (1988).
[19] L. Bryja, A. Wójs, J. Misiewicz, M. Potemski, D. Reuter, and A. Wieck, Phys. Rev. B **75**, 035308 (2007).
[20] A. Wójs, Phys. Rev. B **76**, 085344 (2007).
[21] G. Bartsch, M. Gerbracht, D. R. Yakovlev, J. H. Blokland, P. C. M. Christianen, E. A. Zhukov, A. B. Dzyubenko, G. Karczewski, T. Wojtowicz, J. Kossut, J. C. Maan, and M. Bayer, Phys. Rev. B **83**, 235317 (2011).
[22] I. A. Yugova, A. Greilich, D. R. Yakovlev, A. A. Kiselev, M. Bayer, V. V. Petrov, Y. K. Dolgikh, D. Reuter, and A. D. Wieck, Phys. Rev. B **75**, 245302 (2007).
[23] M. Kubisa, L. Bryja, K. Ryczko, J. Misiewicz, C. Bardot, M. Potemski, G. Ortner, M. Bayer, A. Forchel, and C. B. Sørensen, Phys. Rev. B **67**, 035305 (2003).
[24] *Numerical Data and Functional Relationships in Science and Technology*, Landolt-Börnstein, New Series, Group III, Vol. 17, edited by O. Madelung (Springer, Berlin, 1982).
[25] S. R. Eric Yang and L. J. Sham, Phys. Rev. Lett. **58**, 2598 (1987).
[26] R. P. Leavitt and J. W. Little, Phys. Rev. B **42**, 11774 (1990).
[27] P. Peyla, R. Romestain, Y. Merle d'Aubigné, G. Fishman, A. Wasiela, and H. Mariette, Phys. Rev. B **52**, 12026 (1995).